Journal of Cellular Biochemistry 103:1101–1110 (2008)

NCX3 Is a Major Functional Isoform of the Sodium–Calcium Exchanger in Osteoblasts

Donna M. Sosnoski* and Carol V. Gay

The Pennsylvania State University, Department of Biochemistry and Molecular Biology, University Park, Pennsylvania 16802

Abstract The calcium phosphate-based skeleton of vertebrates serves as the major reservoir for metabolically available calcium ions. The skeleton is formed by osteoblasts which first secrete a proteinaceous matrix and then provide Ca^{++} for the calcification process. The two calcium efflux ports found in most cells are the plasma membrane Ca-ATPase (PMCA) and the sodium–calcium exchanger (NCX). In osteoblasts, PMCA and NCX are located on opposing sides of the cell with NCX facing the mineralizing bone surface. Two isoforms of NCX have been identified in osteoblasts NCX1, and NCX3. The purpose of this study was to determine the extent to which each of the two NCX isoforms support delivery of Ca^{++} into sites of calcification and to discern if one could compensate for the other. SiRNA technology was used to knockdown each isoform separately in MC3T3-E1 osteoblasts. Osteoblasts in which either NCX1 or NCX3 was impaired were tested for Ca^{++} efflux using the Ca^{++} specific fluorophore, fluo-4, in a sodium-dependent calcium uptake assay adapted for image analysis. NCX3 was found to serve as a major contributor of Ca^{++} translocation out of osteoblasts into calcifying bone matrix. NCX1 had little to no involvement. J. Cell. Biochem. 103: 1101–1110, 2008.

Key words: NCX1; NCX3; osteoblasts; sodium–calcium exchange

Intracellular calcium homeostasis is crucial for the function of all cells. Calcium ions enter cells through a variety of gated channels and exit cells by the plasma membrane Ca^{++}-ATPase (PMCA) and the Na^{+}/Ca^{++} exchanger (NCX) [Carafoli, 1987]. In osteoblasts, both PMCA and NCX are asymmetrically located; PMCA faces the bone marrow compartment [Akisaka et al., 1988; Watson et al., 1989] and NCX faces the bone surface [Stains and Gay, 1998]. Because of their locations, NCX is poised to extrude Ca^{++} into newly formed bone matrix whereas PMCA is not likely to play a direct role in mineralization.

Delivery of calcium ions into mineralizing osteoid is one of the main functions of bone-forming osteoblasts and is the focus of the present study. The discovery of the opposing locations of PMCA and NCX prompted us to investigate the function of NCX in osteoblasts.

The first report demonstrating the presence of NCX in bone tissue came from organ culture experiments by Krieger and Tashjian [1980]. Subsequent reports have revealed the presence of NCX in primary osteoblasts and in an osteoblast-like cell line, UMR-106 [Krieger, 1992; Short et al., 1994]. The NCX1 isoform has been reported for UMR-106 osteoblasts [White et al., 1996] and in primary osteoblasts [Stains et al., 2002].

Localization of NCX by immunohistochemical staining of cultures of primary osteoblasts revealed NCX on the cell surface which faces newly formed bone matrix, that is, osteoid [Stains and Gay, 1998]. When NCX was specifically inhibited, mineralization of matrix produced in vitro by primary osteoblasts was substantially diminished [Stains and Gay, 2001]. Stains et al. [2002] also investigated the expression of the two most likely NCX isoforms, NCX1 and NCX3, in osteoblasts and found that

Grant sponsor: U.S. Army Medical Research and Materiel Command; Grant number: DAMD 17-03-1-0583; Grant sponsor: National Institutes of Health; Grant number: DE 09459.

*Correspondence to: Donna M. Sosnoski, The Pennsylvania State University, Department of Biochemistry and Molecular Biology, 432 South Frear Building, University Park, PA 16802. E-mail: dms28@psu.edu

Received 18 April 2007; Accepted 15 June 2007

DOI 10.1002/jcb.21483

both are present, with NCX3 being more abundant.

The present study has focused on determining which isoform is responsible for the transport of calcium into mineralizing sites of newly formed bone matrix. We have determined that NCX3 is the predominant isoform that supports calcium extrusion into sites of calcification.

MATERIALS AND METHODS

Cell Culture

The mouse osteoblastic cell line MC3T3-E1 was routinely propagated in alpha MEM (MediaTech, Herndon, VA) supplemented with 10% fetal bovine serum (Sigma, St. Louis, MO) and 1% penicillin/streptomycin (MediaTech) and incubated at 37°C in a 5% CO_2 humidified atmosphere. For timecourse differentiation experiments, cells were plated at a density of 2×10^4 cells per square centimeter in 35 and 60 mM dishes in alpha MEM, 10% FBS, 1% penicillin streptomycin, 10 mM β-glycerophosphate (Sigma) and 50 μg/ml ascorbic acid (Aldrich Chemical, Milwaukee, WI). Cells plated at this density were confluent by day 4. Cells were cultured at 37°C 5% CO_2 for requisite number of days with media replacement every 3 days.

RT-PCR of NCX-1, NCX-3, Cadherin 11, and Connexin 43

A 60 mm dish of MC3T3-E1 cells was harvested at the time intervals shown in Figures 2 and 3; total RNA was isolated from the cells using the RNeasy Mini kit (Qiagen, Valencia, CA) with on-column DNase treatment. One microgram of total RNA was reverse transcribed from an oligo dT primer using the RETROscript kit (Ambion, Austin, TX). One-tenth of this reaction was used in relative quantitative PCR reactions to determine the levels of message for each of the proteins of interest. Levels of amplified PCR product were normalized to 18S RNA using QuantumRNA 18S internal standard primers (Ambion). PCR reactions were optimized by varying the cycle number to determine the linear range of the amplification. RNA that had not been reverse transcribed was used as a negative control. PCR reactions for each of the proteins of interest were performed using the forward and reverse primers and cycle numbers listed in Table I. Thermocycler parameters for all reactions were: 95°C for 30 s, 60°C for 30 s, and 72°C for 1 min. PCR products were separated by electrophoresis on a 1.5% agarose gel in 1× tris borate EDTA buffer and stained with ethidium bromide. Gel documentation was performed by the Kodak Gel Logic 100 Imaging System (Eastman Kodak, Rochester, NY) and band volume quantitation was done by ImageQuant software (Molecular Dynamics, Sunnyvale, CA).

Alkaline Phosphatase Activity Assay

At the designated time intervals, a 35 mm dish of MC3T3-E1 cells was rinsed twice with phosphate buffered saline (PBS) and lysed in buffer consisting of 100 mM glycine, 1 mM $MgCl_2$ and 0.1% Triton X-100, pH 10.0 for 10 min at 4°C. Lysates were assayed by a quantitative kinetic alkaline phosphatase assay kit (Sigma) and the data normalized with respect to total protein content of each sample.

Von Kossa Staining

MC3T3-E1 osteoblasts cultured for the requisite number of days were stained for matrix mineralization by the Von Kossa method. Briefly, cells were rinsed once with

TABLE I. Primers, Cycle Number and Amplicon Size for Relative Quantitative RT-PCR

Gene	Primer sequence	Cycle #	Amplicon size (bp)	Citations
NCX1	5′ ttgttttcccatgttgacca 3′ 5′ aagttatggccgcacacttc 3′	25	407	[a]
NCX3	5′ ctgcaaggagggtgtcattt 3′ 5′ aaagactcgcaggtgcttgat 3′	27	450	[a]
Cadherin 11	5′ cgtggagggttcagtcggcaga 3′ 5′ tactgatactcaggtttgat 3′	23	436	[b]
Connexin 43	5′ gtcagcttggggtgatgaacag 3′ 5′ atggttttctccgtgggacg 3′	20	498	[c]

Primer3 software developed by the Whitehead Institute for Biomedical Research.
[a]Primers designed from Genbank sequence AF004666 (NCX1) and NM_080440 (NCX3) with.
[b]Kawaguchi et al. [2001].
[c]Chung et al. [1999].

PBS then fixed for 10 min in 10% neutral-buffered formalin. The cells were incubated in the dark for 30 min in 5% silver nitrate, rinsed three times with ddH_2O and then exposed to ambient light for color development. Images of the mineralized areas were collected using light microscopy.

siRNA Design and Synthesis

SiRNA oligonucleotide templates were designed by using the Ambion on-line program, siRNA Target Finder (www.ambion.com/techlib/misc/siRNA-finder.html) and the Genbank mRNA sequence for NCX-1 (accession AF004666) and NCX-3 (accession NM_080440). Three siRNA templates targeted to the 5′ region of the mRNA were chosen for each NCX isoform (Fig. 1). An additional siRNA template was created for NCX1 that was targeted to the central region of the mRNA. Template oligonucleotides were synthesized by MWG Biotech (High Point, NC) and utilized in the generation of double stranded siRNA constructs by the Ambion Silencer siRNA construction kit. Control template oligonucleotides included in the kit provided a siRNA construct to GAPDH that was used as a control in subsequent experiments. Briefly, an 8 nt 5′ leader was synthesized as part of the sense and antisense strands of the template oligonucleotides. A T7 promoter primer was annealed to the leader to enable transcription of the sense and antisense templates by T7 RNA polymerase. The two strands were then hybridized into a double-stranded RNA; the single-stranded overhanging leader sequences were removed by digestion with RNase. The resulting double-stranded siRNA construct was purified by glass fiber filter binding and elution. Yields of siRNA were quantitated by spectrophotometric readings at an absorbance wavelength of 260 nm.

siRNA Transfection

The MC3T3-E1 osteoblast cells were grown to 60–80% confluency (in 3 days) in 35 mm glass bottom microwell dishes (MatTek, Ashland, MA). The 35 mm culture dish contained a 14 mm circular culture area enclosed on the bottom with a 1.5 mm glass coverslip. This configuration allowed for superior optical quality for the confocal imaging to follow. Four micrograms of each siRNA construct was combined with 37.5 μl of the polyamine transfection reagent SuperFect (Qiagen) in 125 μl of alpha MEM and incubated at room temperature for 10 min. After addition of 750 μl of alpha MEM with 10% FBS, the transfection cocktail was applied to a 35 mM dish of MC3T3-E1 cells that

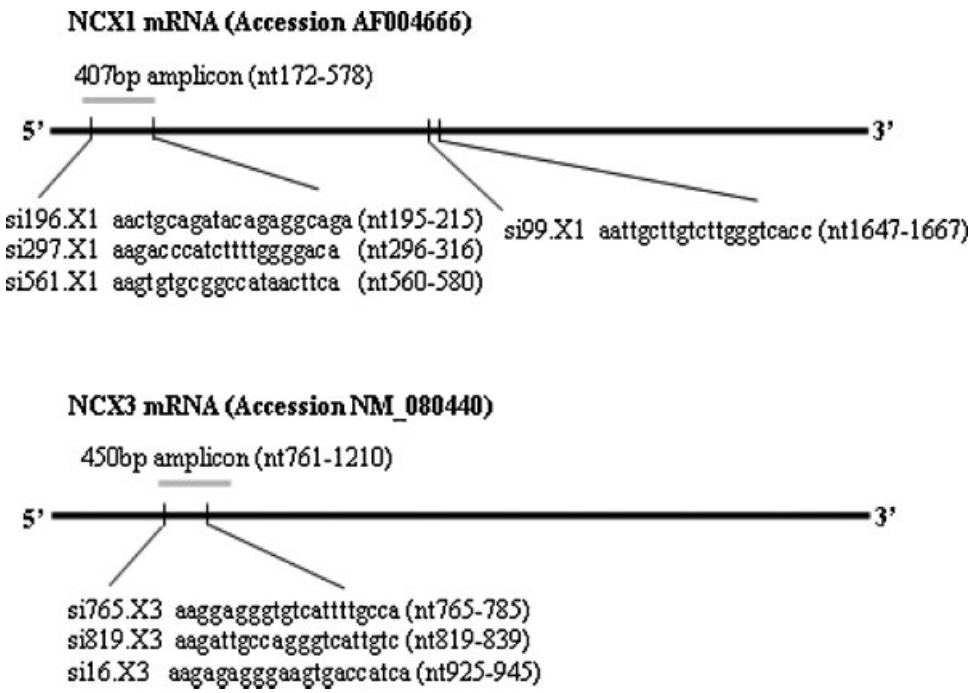

Fig. 1. Schematic representation of short interfering RNA constructs for mouse NCX1 and NCX3. Gray bar denotes location and size of RT-PCR amplicon.

had been rinsed twice with PBS. Plates were incubated at 37°C 5% CO_2 for 2 h. The transfection mix was then removed and replaced with osteoblast differentiation medium consisting of alpha MEM, 10% FBS, 0.1% pen/strep, 10 mM β-glycerophosphate and 50 μg/ml ascorbic acid. Cultures were fed fresh media the following day and every other day thereafter. For Western blot analysis, the MC3T3-E1 cells were grown in 60 mM tissue culture dishes. The transfection protocol was followed as above with the exception that all volumes for transfection cocktail reagents were increased threefold to accommodate the increase number of cells present in the larger culture plate. All transfections were done in duplicate for each experiment.

Western Blotting

Three days after transfection of the siRNAs, the MC3T3-E1 osteoblast cultures were rinsed twice with PBS containing 1 μg/ml leupeptin (Sigma), 1 μg/ml pepstatin (Sigma), 10 μg/ml PMSF (Sigma) and 0.5 mM EDTA. These protease inhibitors were also present in all subsequent solution to inhibit degradation of proteins in the lysate. Cells were then scraped into 2 ml of the PBS solution, centrifuged and resuspended in 35 μl of PBS with protease inhibitors and 0.5% TritonX-100. The cell lysate was sonicated for 1 min and chilled on ice for 1 min; this procedure was repeated a total of four times. The lysate was then centrifuged at 7,000 rpm for 10 min and the supernatant removed to a fresh tube for storage at −80°C. Total protein concentration was determined by the Bradford method (Bio-Rad, Hercules, CA).

Twenty-five micrograms of each protein sample were denatured and separated on an 8% SDS–PAGE gel then transferred onto Immobilon-P PVDF membrane (Millipore Corp., Bedford, MA). Membranes were blocked in a solution of 5% non-fat dry milk (NFDM) in tris-buffered saline with 0.1% Tween-20 (TBS-T). Since the sequence for NCX is highly conserved across species [Kofuji et al., 1992], we utilized a polyclonal rabbit antibody raised against canine cardiac sarcolemma (Research Diagnostics, Inc., Flanders, NJ), at a dilution of 1:500. The control antibody for β-actin (Sigma) was diluted 1:2,000. Due to 74% homology between NCX1 and NCX3, the NCX antibody was used to detect both isoforms. Both primary antibodies were diluted in TBS-T 1% NFDM and incubated with the membranes at 4°C overnight. After washing the membranes in TBS-T 3×20 min at room temperature, the secondary antibody, a donkey anti-rabbit IgG conjugated to horseradish peroxidase (Amersham, Cleveland, OH), was applied at a 1:10,000 dilution and incubated with the membranes for 2 h a room temperature. Blots were then washed 3×20 min. Immunoreactions were detected using the ECL Western blotting analysis system (Amersham) and exposed to autoradiographic film. Band densitometry was performed using ImageQuant software.

Intracellular Calcium Flux Assay

Using a modified procedure from Stains and Gay [1998], Na^+-dependent Ca^{++} uptake was employed to analyze NCX function after transfection of the siRNA constructs for NCX1 and NCX3. MC3T3-E1 cells were cultured for 3 days after transfection with siRNAs. Transfected cells were rinsed twice with a high sodium HEPES buffer (HSHB) consisting of 140 mM NaCl, 10 mM HEPES, 5 mM KCl, 1 mM $MgCl_2$, 10 mM glucose, and 0.1% bovine serum albumin. Cells were then loaded with the calcium indicator dye fluo-4 AM (Molecular Probes, Eugene, OR) by adding 1 ml of loading solution comprised of HSHB, 0.3 mM ouabain (Sigma), 5 μM fluo-4 AM, 0.02% pluronic acid (Molecular Probes), and 1.25 mM probenecid (Molecular Probes). Cells were incubated for 30 min at 37°C then washed 3×5 min in HSHB with 0.3 mM ouabain and 1.25 mM probenecid and incubated an additional 15 min in the solution to allow for complete esterase cleavage of the fluo-4. Cells were then rinsed twice with a low sodium HEPES (LSHB) assay buffer consisting of 5 mM NaCl, 135 mM choline chloride, 10 mM HEPES, 5 mM KCL, 1 mM $MgCl_2$, 10 mM glucose and 0.1% BSA. After the final wash, 250 μl of LSHB assay buffer was added to the glass-bottom center well and the dish was placed on the microscope stage. Ca^{++} flux was monitored with a Bio-Rad MRC 1024 confocal laser microscope (Bio-Rad) using a 32× objective lens and LaserSharp 2000 time course software. A baseline fluorescence reading was measured for 1 min. A 5 μl bolus of 60 mM $CaCl_2$ was then added to the assay buffer on the cells. Calcium influx was then determined by the changes in relative pixel intensity for the 0.121 mm^2 optical field which contained approximately 150 cells. Fluorescence readings were obtained every 5 s for a total of 5 min.

Calcium flux assays were performed for NCX1, NCX3, and control constructs within the same experiment.

RESULTS

Timecourse of mRNA Expression in MC3T3-E1 Osteoblasts

Message for NCX1 was present by 8 days of culture, was highest at 16 days, and tapered off gradually as time in culture progressed (Fig. 2A). NCX3 message also was present at 8 days, peaked at 16 days but tapered off more quickly than occurred for NCX1 (Fig. 2B). The ratios of 18S primer/competimers used (1:12 for NCX1 and 1:15 for NCX3) indicate that transcripts for both NCX1 and NCX3 are relatively rare. On the other hand, cadherin 11 and connexin 43 messages were expressed throughout the culture time course and were present in substantial amounts by day 8 (Fig. 2C,D). The primer:competimer ratios used for cadherin 11 and connexin 43 were 1:8 and 1:9, respectively, suggesting more abundant transcripts. Alkaline phosphatase activity, a marker of osteoblast differentiation, was detectable by day 4, peaked by day 16 and continued to be expressed throughout the entire culture period (Fig. 3). The MC3T3-E1 cell cultures were also stained for the presence of mineralized matrix by the von Kossa method. Mineralization was detected as early as day 16 and continued to accumulate throughout the culture period (data not shown).

Knockdown of NCX Protein by siRNA

Reductions of NCX protein in the MC3T3-E1 cells that had been transfected with siRNA to NCX1, NCX3, or GAPDH were assessed by Western blot. As shown in Figure 4, when NCX1 siRNAs were used NCX protein expression was reduced 50–60%. Constructs for NCX3 resulted in a 20–30% reduction of NCX. This experiment shows that the siRNA constructs employed were successful in reducing the amount of sodium–calcium exchanger present in the plasma membrane of the mouse osteoblast cells.

Knockdown of NCX1 and NCX3 Function

To demonstrate which NCX isoform is responsible for calcium efflux in MC3T3-E1 osteoblasts, siRNA constructs designed to knockdown expression of NCX1 or NCX3 were transfected into the cells and sodium-dependent calcium uptake assays were performed.

Figure 5 shows typical fields of view from which levels of intracellular Ca^{++} uptake were assayed by monitoring the levels of fluorescence

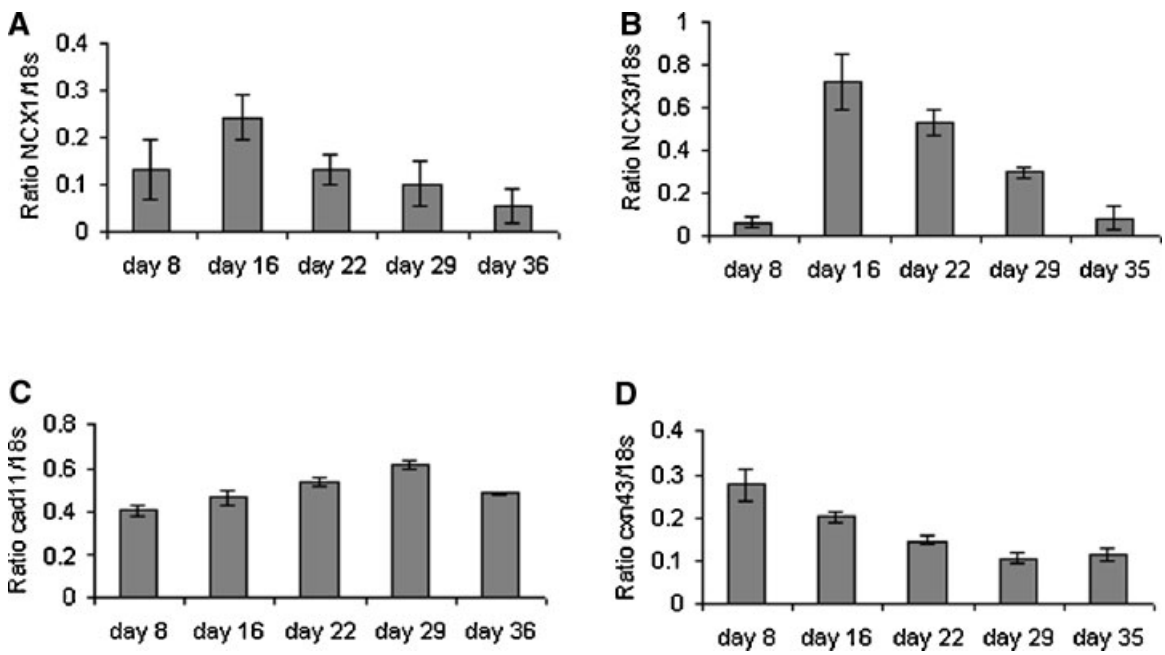

Fig. 2. Time course of mRNA expression of NCX1 (**A**), NCX3 (**B**), cadherin-11 (**C**), and connexin-43 (**D**) as determined by relative quantitative RT-PCR in differentiating MC3T3-E1 osteoblasts. Error bars denote standard deviation where n = 3.

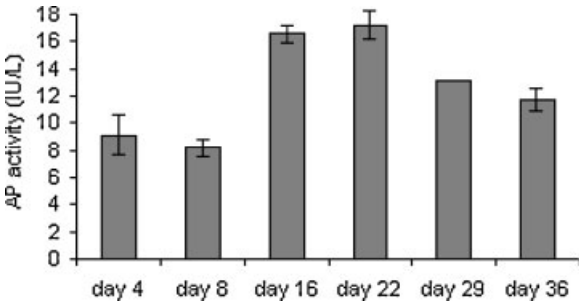

Fig. 3. Time course of alkaline phosphatase activity in differentiating MC3T3-E1 osteoblasts. Error bars denote standard deviation where n = 3.

from the calcium indicator fluo-4. The phase contrast images (left hand column) show that fields evaluated consisted of a confluent monolayer of cells. The central column in Figure 5 shows the baseline level of fluorescence prior to addition of extracellular Ca^{++}. The right-hand column records images at peak fluorescence 195 s after introducing the bolus of Ca^{++}. Fluorescence for the GAPDH (Fig. 5C) and siRNA knockdown of NCX1 (Fig. 5F) is similar. When NCX3 was knocked down fluorescence was substantially diminished (Fig. 5I). Figure 6 graphs the time course of Ca^{++} uptake by cells which had been transfected by GAPDH, by siRNAs 297.X1 and 196.X1 to knockdown NCX1, and by siRNAs 819.X3 and 16.X3 to

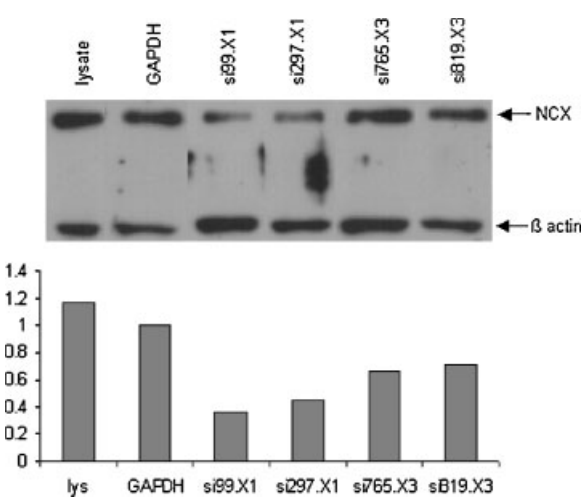

Fig. 4. Western blot analysis of NCX protein in MC3T3-E1 cells transfected with siRNAs to NCX1 (99.X1 and 297.X1) or NCX3 (765.X3 and 819.X3). Bar graph shows amounts of NCX protein (normalized to β-actin) relative to amount expressed in control cells transfected with a short interfering RNA to GAPDH. Protein sample in the lane designated as lysate was extracted from untransfected cells. Calcium flux assays were simultaneously performed on this same batch of transfected cells.

knockdown NCX3. When NCX1 was knocked down Ca^{++} influx was minimally altered, as compared to the GAPDH control. NCX3 knockdown resulted in about a 50% reduction of Ca^{++} uptake. Table II provides a summary of calcium uptake results for the various siRNA constructs employed in this study. It is noteworthy that all three NCX3 constructs substantially diminished Ca^{++} uptake while all four NCX1 constructs had a minimal impact on Ca^{++} flux.

DISCUSSION

Three isoforms of the sodium–calcium exchanger have been identified in vertebrates NCX1 [Nicoll et al., 1990], NCX2 [Li et al., 1994] and NCX3 [Nicoll et al., 1996]. For these exchangers, Ca^{++} efflux occurs in exchange for Na^{+} and the process is regulated in part by intracellular Ca^{++} levels. NCX1 appears to be ubiquitously expressed in all tissues but is in greatest abundance in excitable cells, whereas NCX2 and NCX3 have a much narrower distribution [Matsuoka, 2004]. There appears to be little functional difference among NCX1, NCX2, and NCX3 [Linck et al., 1998]. However, a number of mechanisms exist for regulating sodium–calcium exchange, with some types of regulation being isoform specific [Philipson and Nicoll, 2000; Matsuoka, 2004; DiPolo and Beauge, 2006]. It is particularly interesting that the sodium–calcium exchanger is up-regulated by TGF-β1 and dexamethasone [Smith and Smith, 1994; Carrillo et al., 1998] as these two substances have profound stimulatory effects on osteoblasts.

Brain and central nervous system are the only vertebrate tissues known to express all three exchangers. The distributions of NCX1, NCX2, and NCX3 are distinct within the brain, suggesting differences in function and regulation [Canitano et al., 2002]. NCX1 is present in high levels in brain, heart and kidney and in lower amounts in skeletal muscle [Iwamoto, 2004] and non-excitable cells including osteoblasts and odontoblasts [Lundquist et al., 2000; Stains et al., 2002]. NCX1 has several splice variants and these also have tissue specific distribution patterns [Schulze et al., 2002]. For example, transcripts in which exon-A sequences are transcribed appear mainly in excitable cells; transcripts derived from exon-B sequences appear in non-excitable cells. The role of NCX1 is typically to maintain appropriate levels of

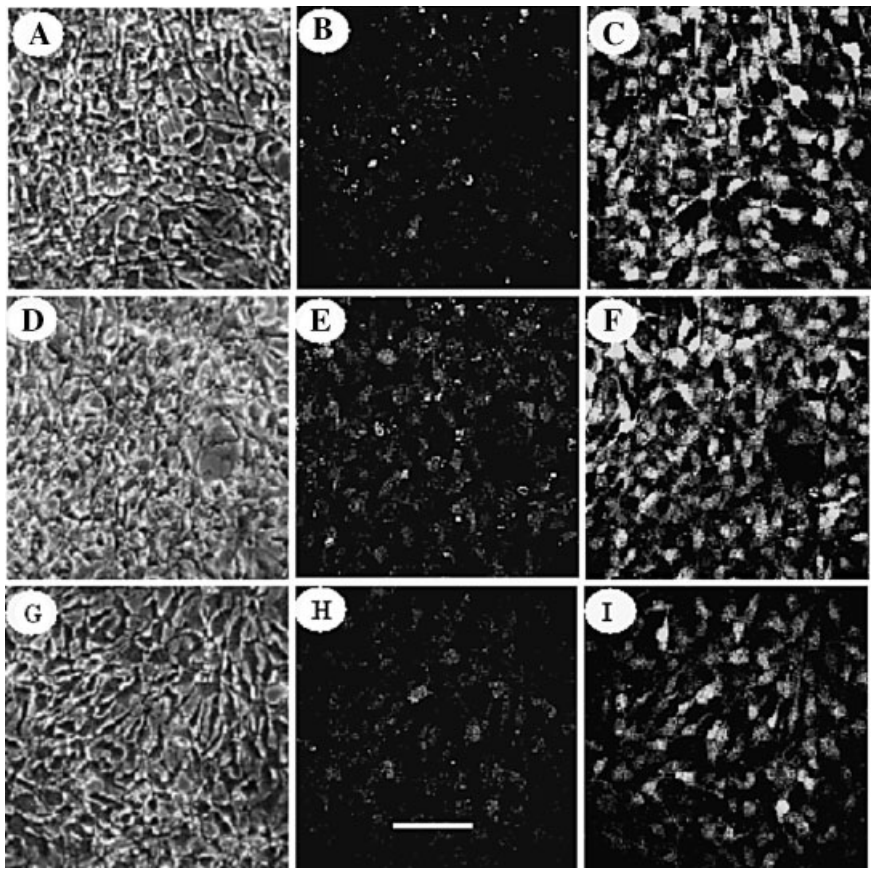

Fig. 5. Confocal imaging of Na^{+}-dependent Ca^{++} flux in MC3T3-E1 osteoblasts tranfected with siRNA constructs to GAPDH (**A**–**C**), NCX-1 (**D**–**F**), and NCX3 (**G**–**I**). Phase contrast images (A, D, and G) show confluency of each field; images (B, E, and H) show baseline fluorescence before the addition of the Ca^{++} bolus. Images (C, F, and I) show the peak level of fluorescence 195 s after addition of calcium to the assay buffer. Scale bar = 100 μm.

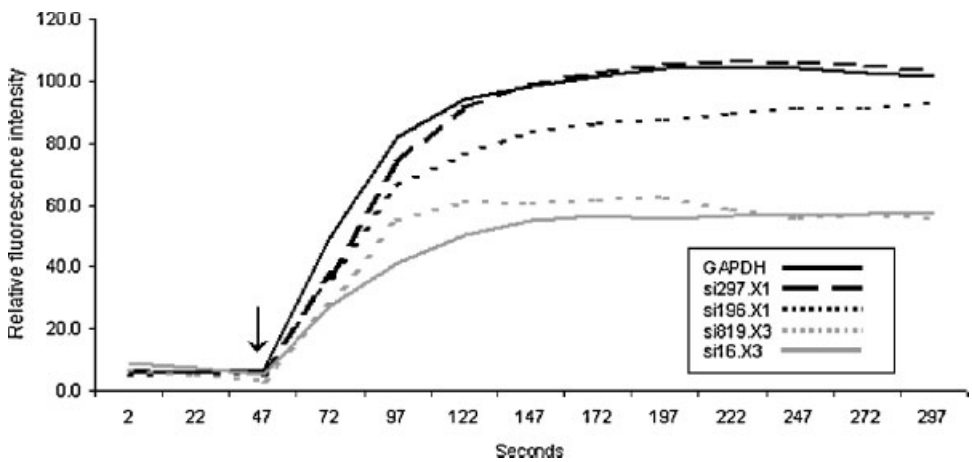

Fig. 6. Na^{+}-dependent Ca^{++} uptake in MC3T3-E1 cells transfected with siRNA constructs to NCX1 and NCX3. Plots represent the average change in pixel intensity of the calcium sensitive dye fluo-4 for the entire field of cells. Arrow indicates the time point at which a bolus of 1.5mM $CaCl_2$ was added to the cell assay chamber.

TABLE II. NCX Functional Knockdown by siRNAs as Determined by Na^+-Dependent Calcium Uptake

siRNA construct	% of control siRNA	n
196.X1	83 ± 3.5 s.d.	4
297.X1	73.5 ± 8.9 s.d.	6
561.X1	86.5 ± 11.7 s.d.	4
99.X1	74.8 ± 6.1 s.d.	5
16.X3	60.5 ± 9.8 s.d.	4
765.X3	45 ± 17.7 s.d.	6
819.X3	56 ± 8.1 s.d.	6

intracellular Ca^{++}. In contrast to NCX1, NCX2 has been reported in brain and skeletal muscle only [Quednau et al., 1997]. NCX3 has been reported in brain, skeletal muscle [Quednau et al., 1997], osteoblasts [Stains and Gay, 1998; Stains and Gay, 2001; Stains et al., 2002], and mast cells [Aneiros et al., 2005]. Two splice variants are known to exist for NCX3 [Quednau et al., 1997].

In the present study, we found that the MC3T3-E1 cell line achieved the differentiated state by 16 days. At this time alkaline phosphatase activity had peaked as well as the expression of NCX1 and NCX3. We also monitored cadherin 11, also termed osteoblast cadherin, and the gap junction protein, connexin 43. Connexin 43 was abundantly expressed by culture day 8, suggesting that gap junctions form early in osteoblast development and are sustained throughout the culture period. This enables osteoblasts to communicate with each other as signaling molecules pass from cell to cell. Expression of cadherin 11 also appeared early in osteoblast development and expression continued to be expressed at approximately the same level throughout the culture period. The continued expression of these three proteins (alkaline phosphatase, connexin 43, and cadherin 11), all of which are important for osteoblast function, is an indication that the osteoblast phenotype was maintained throughout the culture period.

The goal of this study was to evaluate function of the two NCX isoforms found in osteoblasts. We found both NCX1 and NCX3 isoforms in the MC3T3-E1 cells as expected since both of those exchangers had been demonstrated in primary osteoblasts [Stains et al., 2002]. We used MC3T3-E1 cells, rather than primary osteoblasts, in order to provide a more predictable model for transfection with siRNA. We developed a set of siRNAs to knock down expression of both isoforms. In NCX knockdown experiments done with antisense oligodeoxynucleotides targeted to the 5′ coding region, Slodzinski and Blaustein [1998] demonstrated successful reduction of NCX function in cardiac myocytes. Other research has shown that a functionally active 70 kDa N-terminal (5′) form of NCX exists [Saba et al., 1999; Van Eylen et al., 2001]. In order to maximize the knockdown effect of the siRNA to NCX1 and NCX3, we concentrated on targeting the 5′ coding region of both messages. Western blot analysis demonstrated that the siRNAs designed to block the synthesis of NCX1 or NCX3 yielded a substantial reduction in NCX protein expression. It is possible that the polyclonal antibody used to detect both NCX bands may have had differing affinities for each isoform and so the changes in band densities are only a qualitative assessment. Nonetheless, it is clear that knock down occurred for both isoforms at the protein level.

To examine the contribution of NCX1 and NCX3 to Ca^{++} extrusion by osteoblasts, we introduced a fluorophore specific for Ca^{++} into the osteoblasts. Addition of a bolus of Ca^{++} to the low sodium assay medium forced the Na–Ca exchanger to operate in reverse mode, that is, Ca^{++} entered the cell instead of being extruded. The stoichiometry of the forward and reverse modes and other characteristics of the NCX isoforms are similar, as recently reviewed by DiPolo and Beauge [2006]. As shown in Table II, when NCX1 was knocked down by four different siRNAs, calcium uptake was only slightly affected. However, Ca^{++} uptake was substantially reduced by three different constructs for NCX3. Correlated with this observation is the earlier demonstration that NCX3 is more abundant than NCX1 in osteoblasts [Stains et al., 2002]. Collectively, these data indicate that NCX3 is the predominant isoform in osteoblasts that supports calcium extrusion to the bone matrix.

One concern we had was if the 3-day time interval between introduction of the siRNAs and Ca^{++} flux measurement was sufficiently long to affect the amount of NCX protein in the plasma membrane. In a study using antisense oligonucleotide technology, NCX turnover was found to be more rapid than the typical turnover rate for many plasma membrane proteins [Egger et al., 2005]. For example, in primary neurons turnover has been reported to

be 12–24 h [Ranciat-McComb et al., 2000]. Additionally, Western blot analysis in the present study confirms a reduction in the amount of NCX protein 3 days after transfection with siRNA.

One question we sought an answer for was if one exchanger could compensate for the other. Our data suggest that such compensation does not occur. When NCX3 was knocked down, calcium flux was reduced, even though the functional NCX1 was still present. NCX1 did not appear to be upregulated to compensate for the lack of NCX3. Supporting our data is a study by Wakimoto et al. [2003] in which it was shown that neither NCX2 nor NCX3 protein levels were increased to compensate for the NCX1 deficiency in the brain tissue of heterozygous knockout mice.

The finding in this study that reduced NCX3 protein expression resulted in substantial reduction in Ca^{++} flux correlates with earlier data which revealed that deposition of calcium phosphate crystals into bone matrix was markedly impaired when inhibitors of NCX were present. In the 2001 study, Stains and Gay [2001] demonstrated that the NCX inhibitor, KB-R7943, was the most effective in preventing mineralization. It is now known that KB-R7943 is particularly effective in inhibiting NCX3 [Iwamoto, 2004]. It had been previously demonstrated that the Na–Ca exchanger is positioned in osteoblasts on the matrix producing side of the cell [Stains and Gay, 1998]. At that time, only a polyclonal antibody was available for immunocytochemical localization and so the presence of NCX1 and/or NCX3 could not be deduced. Collectively, the present study along with the earlier work indicates that the NCX3 isoform is positioned appropriately and functions as the major portal for translocation of calcium ions into sites of mineralization. Other sodium–calcium exchangers have been found in close proximity to sites where Ca^{++} extrusion has an immediate effect, as reviewed by Reeves [1998].

ACKNOWLEDGMENTS

This work was supported by The National Institutes of Health, Grant number DE 09459. We wish to thank Dr. Norman Karin, University of Delaware, for the kind gift of the MC3T3-E1 cells and Virginia Gilman and Jonathan Kotula for their technical assistance.

REFERENCES

Akisaka T, Yamamoto T, Gay CV. 1988. Ultracytochemical investigation of calcium activated adenosine triphosphate (Ca^{++}-ATPase) in chick tibia. J Bone Miner Res 3:19–25.

Aneiros E, Philipp S, Lis A, Freichel M, Cavalie A. 2005. Modulation of Ca^{2+} signaling by Na^{+}/Ca^{2+} exchangers in mast cells. J Immunol 174:119–130.

Canitano A, Papa M, Boscia F, Castaldo P, Sellitti S, Taglialatela M, Annunziato L. 2002. Brain distribution of the Na^{+}/Ca^{2+} exchanger-encoding genes NCX1, NCX2, and NCX3 and their related proteins in the central nervous system. Ann NY Acad Sci 976:394–404.

Carafoli E. 1987. Intracellular calcium homeostasis. Annu Rev Biochem 56:395–433.

Carrillo C, Cafferata EG, Genovese J, O'Reilly M, Roberts AB, Santa-Coloma TA. 1998. TGF-beta1 up-regulates the mRNA for the Na^{+}/Ca^{2+} exchanger in neonatal rat cardiac myocytes. Cell Mol Biol (Noisy-le-grand) 44:543–551.

Chung CY, Iida-Klein A, Wyatt LE, Rudkin GH, Ishida K, Yamaguchi DT, Miller TA. 1999. Serial passage of MC3T3-E1 cells alters osteoblastic function and responsiveness to transforming growth factor-beta1 and bone morphogenetic protein-2. Biochem Biophys Res Commun 265:246–251.

DiPolo R, Beauge L. 2006. Sodium/calcium exchanger: Influence of metabolic regulation on ion carrier interactions. Physiol Rev 86:155–203.

Egger M, Porzig H, Niggli E, Schwaller B. 2005. Rapid turnover of the "functional" Na(+)-Ca(2+) exchanger in cardiac myocytes revealed by an antisense oligodeoxynucleotide approach. Cell Calcium 37:233–243.

Iwamoto T. 2004. Forefront of Na^{+}/Ca^{2+} exchanger studies: Molecular pharmacology of the Na^{+}/Ca^{2+} exchange inhibitors. J Pharmacol Sci 96:27–32.

Kawaguchi J, Azuma Y, Hoshi K, Kii I, Takeshita S, Ohta T, Ozawa H, Takeichi M, Chisaka O, Kudo A. 2001. Targeted disruption of cadherin-11 leads to a reduction in bone density in calvaria and long bone metaphyses. J Bone Miner Res 16:1265–1271.

Kofuji P, Hadley RW, Kieval RS, Lederer WJ, Schulze DH. 1992. Expression of the Na-Ca exchanger in diverse tissues: A study using the cloned human Na-Ca exchanger. Am J Physiol 263:C1241–C1249.

Krieger NS. 1992. Demonstration of sodium/calcium exchange in rodent osteoblasts. J Bone Miner Res 7:1105–1111.

Krieger NS, Tashjian AH. 1980. Parathyroid stimulates bone resorption via a Na/Ca exchange mechanism. Nature 287:843–845.

Li Z, Matsuoka S, Hryshko LV, Nicoll DA, Bersohn MM, Burke EP, Lifton RP, Philipson KD. 1994. Cloning of the NCX2 isoform of the plasma membrane Na(+)-Ca^{2+} exchanger. J Biol Chem 269:17434–17439.

Linck B, Qui Z, He Z, Tong Q, Hilgemann DH, Philipson KD. 1998. Functional comparison of the three isoforms of the Na^{+}/Ca^{2+} exchanger (NCX1, NCX2, NCX3). Am J Physiol Cell Physiol 274:C415–C423.

Lundquist P, Lundgren T, Gritli-Linde A, Linde A. 2000. Na^{+}/Ca^{2+} exchanger isoforms of rat odontoblasts and osteoblasts. Calcif Tissue Int 67:60–67.

Matsuoka S. 2004. Forefront of Na^+/Ca^{2+} exchanger studies: Regulation kinetics of Na^+/Ca^{2+} exchangers. J Pharmacol Sci 96:12–14.

Nicoll DA, Longoni S, Philipson KD. 1990. Molecular cloning and functional expression of the cardiac sarcolemmal $Na(+)$-Ca^{2+} exchanger. Science 250:562–565.

Nicoll DA, Quednau BD, Qui Z, Xia YR, Lusis AJ, Philipson KD. 1996. Cloning of a third mammalian $Na(+)$-Ca^{2+} exchanger, N CX3. J Biol Chem 271:24914–24921.

Philipson KD, Nicoll DA. 2000. Sodium-calcium exchange: A molecular perspective. Annu Rev Physiol 62:111–133.

Quednau BD, Nicoll DA, Philipson KD. 1997. Tissue specificity and alternative splicing of the Na^+/Ca^{2+} exchanger isoforms NCX1, NCX2 and NCX3 in rat. Am J Physiol 272:C1250–C1261.

Ranciat-McComb NS, Bland KS, Huschenbett J, Ramonda L, Bechtel M, Zaidi A, Michaelis ML. 2000. Antisense oligonucleotide suppression of $Na(+)/Ca(2+)$ exchanger activity in primary neurons from rat brain. Neurosci Lett 294:13–16.

Reeves JP. 1998. Na^+/Ca^{2+} exchange and cellular Ca^{2+} homeostasis. J Bioenerg Biomembr 30:151–160.

Saba RI, Bollen A, Herchuelz A. 1999. Characterization of the 70 kDa polypeptide of the Na/Ca exchanger. Biochem J 338:139–145.

Schulze DH, Polumuri SK, Gille T, Ruknudin A. 2002. Functional regulation of alternatively spliced Na^+/Ca^{2+} exchanger (NCX1) isoforms. Ann N Y Acad Sci 976:187–196.

Short CL, Monk RD, Bushinsky DA, Krieger NS. 1994. Hormonal regulation of $Na(+)$-$Ca(2+)$ exchange in osteoblast-like cells. J Bone Miner Res 9:1159–1166.

Slodzinski MK, Blaustein MP. 1998. Physiological effects of Na^+/Ca^{2+} exchanger knockdown by antisense oligodeoxynucleotides in arterial myocytes. Am J Physiol 275: C251–C259.

Smith L, Smith JB. 1994. Regulation of sodium-calcium exchanger by glucocorticoids and growth factors in vascular smooth muscle. J Biol Chem 269:27527–27531.

Stains JP, Gay CV. 1998. Asymmetric distribution of functional sodium-calcium exchanger in primary osteoblasts. J Bone Miner Res 13:1862–1869.

Stains JP, Gay CV. 2001. Inhibition of Na^+/Ca^{2+} exchange with KB-R7943 or bepridil diminished mineral deposition by osteoblasts. J Bone Miner Res 16:1434–1443.

Stains JP, Weber JA, Gay CV. 2002. Expression of $Na(+)/Ca(2+)$ exchanger isoforms (NCX1 and NCX3) and plasma membrane $Ca(2+)$ ATPase during osteoblast differentiation. J Cell Biochem 84:625–635.

Van Eylen F, Kamagate A, Herchuelz A. 2001. A new Na/Ca exchanger splicing pattern identified in situ leads to a functionally active 70kDa NH(2)-terminal protein. Cell Calcium 30:191–198.

Wakimoto K, Fujimura H, Iwamoto T, Oka T, Kobayashi K, Kita S, Kudoh S, Kuro-o M, Nabeshima Y, Shigekawa M, Imai Y, Komuro I. 2003. Na^+/Ca^{2+} exchanger-deficient mice have disorganized myofibrils and swollen mitochondria in cardiomyocytes. Comp Biochem Physiol B Biochem Mol Biol 135:9–15.

Watson LP, Kang YH, Falk MC. 1989. Cytochemical properties of osteoblast cell membrane domains. J Histochen Cytochem 37:1235–1246.

White KE, Gesek FA, Friedman PA. 1996. Na^+/Ca^{2+} exchange in rat osteoblast-like UMR 106 cells. J Bone Miner Res 11:1666–1675.